materials

MDPI

Article

A Study of the Possibility of Producing Annealed and Metallized Pellets from Titanomagnetite Concentrate

Andrey N. Dmitriev, Galina Y. Vitkina *, Victor G. Zlobin, Elena A. Vyaznikova, Larisa A. Marshuk, Yulia E. Burova, Roman V. Alektorov and Vladimir V. Kataev

Laboratory of Pyrometallurgy of Reduction Processes, Institute of Metallurgy of the Ural Branch of the Russian Academy of Sciences, 101 Amundsen St., 620016 Ekaterinburg, Russia; andrey.dmitriev@mail.ru (A.N.D.); vjaznikova@mail.ru (E.A.V.); ferro@ural.ru (L.A.M.); menestrelfox@gmail.com (Y.E.B.); alektorov-rv@mail.ru (R.V.A.); kataev.5959@mail.ru (V.V.K.)

* Correspondence: 20procents@mail.ru

Abstract: The current intensive development of steelmaking is being impeded by a scarcity of pure scrap. The potential to replace pure scrap with metallized raw materials that are naturally alloyed with vanadium and titanium, such as annealed unfluxed titanomagnetite pellets, could facilitate the achievement of key objectives in metallurgical development, particularly in the smelting of electric steel. The objective of this research was to produce annealed and metallized pellets from titanomagnetite concentrate under laboratory conditions, with the intention of further processing them as a commercial product in a blast furnace or as an intermediate product for the production of hot briquetted iron (HBI). The results demonstrate that pellets derived from titanomagnetite concentrate exhibit sufficient compressive strength (up to 300 kg/pellet) and a degree of metallization exceeding 90%, which aligns with the requirements for electric steelmaking. The suitability of pellets derived from titanomagnetite concentrate for use in both blast furnaces and metallization processes has been corroborated.

Keywords: processes of titanomagnetite beneficiation; technology; iron ore concentrate production; pellet creation; blast furnace operation; metallization; phase composition; iron ore concentrate properties

check for updates

Citation: Dmitriev, A.N.; Vitkina, G.Y.; Zlobin, V.G.; Vyaznikova, E.A.; Marshuk, L.A.; Burova, Y.E.; Alektorov, R.V.; Kataev, V.V. A Study of the Possibility of Producing Annealed and Metallized Pellets from Titanomagnetite Concentrate. *Materials* **2024**, *17*, 5338. https://doi.org/10.3390/ma17215338

Academic Editor: Piotr Piszczek

Received: 29 September 2024
Revised: 23 October 2024
Accepted: 29 October 2024
Published: 31 October 2024

Copyright: © 2024 by the authors. Licensee MDPI, Basel, Switzerland. This article is an open access article distributed under the terms and conditions of the Creative Commons Attribution (CC BY) license (https://creativecommons.org/licenses/by/4.0/).

1. Introduction

The principal means of producing steel is through the use of pig iron and ferrous scrap derived from both basic oxygen furnaces (BOF) and electric arc furnaces. The production of direct reduction iron (DRI) from iron ore to metallic iron using non-coking coal or natural gas is currently a subject of active research and development. The utilization of DRI is markedly inferior to the consumption of pig iron and scrap. However, a number of factors influence the gradual expansion of both the production and consumption of DRI in steelmaking.

The situation is primarily influenced by the availability of abundant natural gas reserves in conjunction with limited coal reserves, cost-effective electricity generation, and a growing shortage of coking coal and coke. Furthermore, the necessity for natural iron free from impurities to meet rising steel quality demands, limited resources of high-purity ferrous scrap, and a focus on reducing environmental impact further shape the situation.

In addition to the substitution of metallized raw materials for scarce scrap, the intensification of environmental requirements in the global iron and steel industry in recent years has resulted in a surge in demand for premium iron ore raw materials with elevated iron content and minimal impurities. Such products include metallized pellets and hot briquetted iron (HBI). The technology of the direct reduction of iron, which is used in the production of metallized pellets (including DRI and HBI), is regarded as one of the most promising areas for the effective development of global metallurgy.

According to the World Steel Association [1], global production of HBI/DRI during the period from January to May 2024 exceeded 50.81 million tons. Approximately 60% of this production comes from two countries: India, where coal-based technology is widely utilized, and Iran. Russia and Saudi Arabia are the next most prominent producers in terms of production volumes.

A variety of techniques may be employed for the metallization of iron ore materials. The various solid-phase processes for the production of DRI/HBI in different units and utilizing different reducing agents, including gas and solid reducing agents, are outlined in Table 1 [2–4].

Table 1. Methods of metallization.

Type of Reducing Agent	Unit
Reducing gas	Shaft furnaces Midrex, HYL-III, HYL-IV M, Armco, Purofer, Arex, Ghaem, Plasmared, NSC Retorts HYL-I, HYL-II, Hoganas Fluidised bed reactors (FBRs) FINMET, FIOR, Spirex, Circored Rotary kilns FASTMET, ITmk3
Solid reducing agent	Shaft furnaces BL, KINGLOR, METOR, NML Rotary kilns SL/RN, CODIR, ACCAR, DRC, TDR, SIIL, OSIL, Jindal Rotary (hearth) kilns INMETCO, FASTMET, Comet

The American company Midland-Ross developed the direct reduction of iron, a widely used technology, in the mid-1960s. The reduction of iron oxides from pellets or lump ore is conducted in a shaft furnace, where a counter flow of iron-containing material is arranged to descend under its own weight in conjunction with a hot reducing gas. The temperature within the furnace is maintained at a level below that required for the softening of the charge materials [5].

$$Fe_2O_3 + 3H_2 \rightarrow 2Fe + 3H_2O\uparrow, \quad (1)$$

$$Fe_2O_3 + 3CO \rightarrow 2Fe + 3CO_2\uparrow. \quad (2)$$

The reducing gas is hydrogen, which is produced in conjunction with carbon monoxide as a result of the conversion of natural gas in a separate reactor, referred to as a reformer.

$$CH_4 + 2O_2 \rightarrow CO_2 + 2H_2O. \quad (3)$$

Each metallization plant is comprised of a shaft furnace, a natural gas reformer, an inert gas production system, an aspiration system, and auxiliary systems. The shaft furnace is comprised of a feed hopper, an upper gate with a charge distributor, a lower gate, and a pendulum feeder for the discharge of the metallized product. The furnace is divided into three distinct zones, namely a reducing zone, an intermediate zone, and a cooling zone, each of which is characterized by a specific height.

The metallized pellets are cooled to a temperature of between 40 and 50 degrees Celsius in the lower part of the furnace and subsequently discharged by feeders. Following this, the pellets are screened in order to remove any fines. The cooling process is conducted using a gas mixture comprising reducing gases and fume-mine gases. Subsequently, the metallized product is employed in the production of steel, typically within electric arc furnaces. The utilization of waste gas heat is achieved through the use of recuperators, which serve to heat the natural gas and air supplied for fuel combustion in the reformer [5].

The depth of the reduction process can be gauged by the degree of metallization, which is determined by the Equation (4):

$$\varphi_{met} = Fe_{met}/Fe_{total} \cdot 100\%. \quad (4)$$

In this context, the term φ_{met} denotes the degree of metallization, expressed as a percentage. The variables Fe_{met} and Fe_{total} represent the contents of metallic iron and total iron, respectively, in the metallized product.

The MIDREX process is widely regarded as the most reliable and productive direct reduction iron technology in the world. Roughly 80% of global direct reduced iron production is attributed to the MIDREX process and its analogous variants, with natural gas employed as the reducing agent. The remaining 20% is produced in facilities that manufacture sponge iron, a derivative of DRI, using coal.

The resulting metallized pellets, comprising between 90 and 96.97% iron, can be utilized directly in the electric steelmaking process. The storage and transportation of DRI in its original form presents significant challenges, primarily due to its tendency to oxidize rapidly [6]. Consequently, direct iron reduction plants typically incorporate an additional production step, namely hot briquetting. Briquettes of 60–200 cm^3 are not subject to such rapid corrosion and can be stored in open areas and transported over long distances.

The utilization of pellets in the processes of direct iron production [7,8] is subject to rigorous specifications. These specifications include the recommendation and availability of pellets with a FeO content of less than 1.0% and a total iron content exceeding 65%. Additionally, the recommended and available content of the 9–15 mm fraction is set at a minimum of 85%, with a maximum of 50% for the 9–11 mm fraction. Furthermore, the required strength of the pellets must exceed 300 kg/pellet, which is above the standard compressive strength for blast furnace pellets (200–250 kg/pellet) [9,10]. Moreover, the utilization of ore-coal pellets is a recognized phenomenon [11,12].

The following known results and research works on the processes of direct iron production from titanomagnetite raw materials have been identified. The direct reduction of titanomagnetite concentrate was achieved through the utilization of Itmk3 technology, in conjunction with additives at a concentration of 8–10%. The production of metallized pellets with an iron content of 92.9% was achieved through the use of CaF_2 and low-grade coal with an ash content of 35% at a quantity of 15–16%. These pellets are suitable for replacing scrap in electric furnaces [13].

The results presented in Ref. [14] demonstrate that under conditions of a reducing atmosphere and complete carburization, effective separation of the slag and metal phases is achievable. This results in the transfer of over 95% of Fe into the metal phase, while over 90% of Ti remains in the slag.

An increase in process temperature favors the reduction of vanadium oxides, leading to an increase in the mass fraction and degree of V reduction [15].

The Fe–Ti separation efficiency first increases and then decreases with increasing $P(H_2)/P(H_2 + CO)$ [16,17].

An increase in the MgO content has been demonstrated to enhance the vanadium reduction ratio, while achieving a low titanium content in molten iron is contingent upon a MgO content in slag that is below 11% [18].

As the basicity of CaO/SiO_2 increases during the smelting of metallized titanium-magnetite pellets, the reduction factors of Fe, V, and Cr increase, and the transition of TiO_2 into slag first increases and then decreases [19,20].

Two pathways are available for the reduction of iron- and titanium-bearing oxides to metallic iron: the reduction of titanohematite to titanomagnetite, followed by wüstite and finally metallic iron [21]. Similarly, the reduction of pseudobrookite to metallic iron occurs.

The analysis of the mechanisms involved in these processes indicates that the mineral composition and microstructure of the titanomagnetite pellets have a significant influence on their reducing behavior. Furthermore, the properties of the annealed pellets can be enhanced by the addition of ordinary magnetite [22].

It is possible to utilize waste materials containing, for example, cobalt (Co) as an additive to vanadium-containing pellets. The addition of Co_2O_3 promotes aggregation and the diffusion of metallic iron particles [23].

It is also important to note the role of the reducing gas in these processes (CO/H_2 ratio), which allows for achieving a metallization degree above 90% for both metallized magnetite and titanomagnetite pellets [24,25].

Titanomagnetite ores represent a valuable source of not only iron, but also titanium and vanadium, which are in increasing demand within the industrial sector. The complex nature of this ore also makes its extraction more cost-effective and optimizes the recovery of iron and titanium.

The objective of this research is to investigate the potential of utilizing titanomagnetite concentrate as a raw material for the production of iron ore pellets and their subsequent metallization, with the aim of achieving the requisite characteristics for use in both blast furnace and electric steelmaking processes.

2. Materials and Methods

In this study, we examined a low-grade iron ore titanomagnetite concentrate derived from ore enrichment at the deposit, Pervouralsk, Sverdlovsk region, Russian Federation. The ores at the deposit can be classified into two principal categories: massive (solid, 2.2%) and disseminated (97.8%). The most prevalent ore type is the poor disseminated ore, which constitutes the majority of the ores present. The principal ore minerals are titanomagnetite and ilmenite, with minor concentrations of hematite, chalcopyrite, pyrite, bornite, and chalcocite. Non-ferrous minerals are mainly represented by hornblende, pyroxene, plagioclase, and chlorite, with smaller amounts of epidote, garnet, sphene, and spinel. In some cases, rare grains of apatite and veins of calcite are also present. Titanomagnetite is the primary ore mineral.

The initial ore was crushed according to a three-stage scheme to a size of −70 + 0 mm. Subsequently, the crushed ore was subjected to screening on a 10 mm sieve, whereby the products falling within the ranges of −70 + 10 mm and −10 + 0 mm were separated. Both products were then subjected to distinct dry magnetic separation processes, resulting in the production of magnetic products (poor concentrates) and non-magnetic products. Following the upgrading process, which included fine grinding and a two-stage, low-intensity magnetic cleaning procedure, a vanadium titanomagnetite concentrate was produced [26]. The magnetic products were combined to form a total poor iron concentrate with a total iron content of at least 32%.

Two enrichment schemes were investigated and evaluated in laboratory settings to produce iron ore titanomagnetite concentrates, designated as No. 1 (65% Fe_{total}) and No. 2 (68.5% Fe_{total}), both of requisite quality.

To pelletize the iron ore titanomagnetite concentrates, a laboratory drum-type pelletizer was utilized, allowing for adjustments to both the angle of inclination and the speed of rotation. The technical specifications of the pelletizer are outlined in Table 2.

Table 2. Technical specifications of the pelletizer.

Parameter	Unit of Measurement	Parameter Value
Diameter	mm	450
Width	mm	250
Angle of inclination	degree	0–45
Rotational speed	rpm	0–60

The binder used for the pelletization of both batches of pellets was bentonite clay, with an additive concentration of 0.7% by mass. Additionally, up to 5–7% of pure water was employed.

Subsequently, the pellets were dried in a drying cabinet at a temperature of 110 °C for a period of two hours. Following this, the pellets underwent high-temperature firing under the following conditions: heating to 1300 °C in air for 120 min, exposure for 15 min, and cooling with the furnace. The height of the pellet layer in the substrate was maintained

at 25 mm throughout the process. The firing of the dry pellets was conducted in a muffle furnace, which was equipped to adjust and maintain the required heating rate.

The images displayed in Figure 1 illustrate the pellets of standard quality (a) and improved quality (b), respectively.



(**a**) (**b**)

Figure 1. A photograph of the annealed pellets: (**a**) total iron content: 64.5%; (**b**) total iron content: 68.5%.

The chemical analysis was conducted using a titrimetric method. The determination of Fe_{total} was performed in accordance with the standards set forth in the Russian National Standard 32517.1-2013, while the determination of Fe_{met} and FeO was conducted in accordance with the standards set forth in the Russian National Standard R 53657-2009.

The phase composition of the samples was determined using an X-ray diffraction (XRD) instrument, the XRD-7000S (Shimadzu, Kyoto, Japan), with CuKα radiation and a graphite monochromator. The identification of phases was conducted using the PDF4 database, which is maintained by the International Centre for Diffraction Data (ICDD) in Pennsylvania, USA.

To study the mineralogical composition, the samples were subjected to micro-X-ray structure analysis using a scanning electron microscope (SEM) and an optical microscope. The SEM was a model JSM-5900LM, from Jeol Ltd., Akishima, Tokyo, Japan, while the optical microscope was an Olympus GX-51 from Shinjuku, Kyoto, Japan.

The analysis of concentrate particle size (including the smallest diameter, length, and average diameter) and shape was conducted using a Camsizer XT (Retsch Technology GmbH, Haan, Germany) equipped with the X-Change modular system. The standard measurement range was from 1 µm to 3 mm. The imaging duration was 40 s, with an imaging speed of 1:1 and a dispersion pressure of 50 kPa.

Furthermore, samples of the initial concentrate and those resulting from the beneficiation process were dispatched for analysis to ascertain the elemental composition of both the concentrate and its individual grains. Investigations were conducted using an scanning electron microscope, the VEGA LMS (fourth generation with a thermoemission, field-emission cathode), manufactured by TESCAN in the Czech Republic. This was coupled with an energy dispersive analysis attachment, the Xplore30, produced by OXFORD Instruments. This setup enabled the acquisition of SEM images and real-time analysis of the elemental composition.

To comply with the requirements set out in ISO 4700, compression tests were conducted on a universal machine (BT1-FR050THW.A1K, Zwick GmbH, Ulm, Germany) with a displacement speed of 10 mm/min, and the resulting deformation diagram was duly

recorded. Prior to the compression test, the pellets were individually weighed on an electronic scale (ATL-220d4-1, ACCULAB, Nouvelle-France, Mauritius) with an accuracy of ±0.0003 g to determine their mass.

The study of the reducibility of pellets No. 1 (for blast furnace production) was conducted on the unit in accordance with the requirements set forth in the Russian National Standard 17212-84 (ISO 4695 analogue). The method entails the reduction of the sample by carbon monoxide under specified temperature conditions (heating up to 1100 °C), followed by the determination of the degree of reduction based on the results of chemical analysis of the initial and reduced samples or the loss of oxygen mass during reduction. The composition of the reducing gas is CO (33 ± 0.5%) and N_2 (65 ± 0.5%), with a flow rate of reducing gas into the reaction chamber of (30 ± 1) dm^3/min. The heating mode employed for the reduction of the sample is as follows: the sample is heated for the first 40 min at a rate of 15 degrees Celsius per minute up to 600 degrees Celsius, and then for the subsequent 175 min at a rate of 2.86 degrees Celsius per minute up to 1100 degrees Celsius.

The study of strength at low temperature disintegration (LTD) was conducted in accordance with the international standard ISO 13930. The essence of the method is the reducing of the sample by a gaseous reducing agent in a rotating drum at a specified temperature regime, followed by sieving of the test material into size classes (+6.3 mm; +3.15 mm; +0.5 mm; −0.5 mm), which allows for the characterization of its strength properties. The composition of the reducing gas is as follows: CO (20 ± 0.5%), CO_2 (20 ± 0.5%), H_2 (2%), and N_2 (58 ± 0.5%). The temperature of the process is 500 degrees Celsius.

The investigation of the temperature range associated with the softening and melting of pellets was conducted. This technique entails subjecting a sample of the test material to heating in an inert gas environment, with the objective of determining the temperature at which softening commences, as indicated by the immersion of a rigid rod into the sample under the influence of external pressure. Additionally, the technique allows for the delineation of the temperature range encompassing the onset of softening.

The conditions of the metallization process were as follows. The composition of the reducing gas was CO/N_2 at a ratio of 90/10%. The heating and holding temperature was set at 1050 °C, with a heating rate of 10 °C/min and a holding time of 3 to 4 h. The mass of the pellets was 100 g, and the pellets were cooled in a nitrogen medium until reaching 150 °C.

The pellets were loaded into a mesh basket, which was installed in an electric tube furnace. The flow of reducing gas was supplied to the furnace from the bottom to the top. The mass of the pellets was determined both before and after the metallization process. Subsequently, the cooled pellets were prepared for chemical, phase, and mineralogical analyses.

3. Results and Discussion

The chemical composition of the initial concentrate, as well as that of concentrates No. 1 and No. 2, is provided in Table 3.

Table 3. Chemical composition of the materials.

Sample	Content, Mass. %											
	Fe_{total}	Fe_{met}	FeO	CaO	SiO_2	Al_2O_3	MgO	MnO	TiO_2	V_2O_5	S	P
Concentrate No. 1	65.71	-	23.31	1.40	1.94	1.97	0.75	0.17	1.88	0.68	0.010	0.006
Concentrate No. 2	68.79	-	22.85	1.20	1.25	1.30	0.55	0.16	1.35	0.70	0.0079	0.008
Initial concentrate	38.79	-	12.21	6.64	18.34	10.46	6.77	0.24	4.48	0.44	0.093	0.025

The mineralogical composition of the initial concentrate is diverse, with a predominant presence of magnetite (Fe_3O_4) accounting for 51.4%. This phase is identified as a light crystalline structure (Figure 2), indicating its significance in the concentrate's overall mineralogy. In addition to magnetite, the concentrate contains 32.58% layered alumi-

nosilicate structures, specifically chlorite-serpentine, which is represented by the formula $(Mg,Al)(Si,Al)_4O_{10}(OH)_8$. This component highlights the presence of secondary minerals that can influence the concentrate's properties and processing behavior. Plagioclase, a common feldspar mineral with the formula $(Ca,Na)(Si,Al)_4O_8$, is also found within this group. Minor phases include ilmenite ($FeTiO_3$), which is present at up to 7%, and sphene ($CaSiTiO_5$) at up to 2%. These minerals are typically associated with titanium and can play a role in the concentrate's potential applications and value. Additionally, tremolite, characterized by the formula $Ca_2Mg_5Si_8O_{20}(OH)_2$, is observed in minor inclusions, comprising up to 6% of the concentrate. This amphibole mineral may affect the concentrate's physical and chemical properties, particularly in terms of its thermal stability and reactivity.

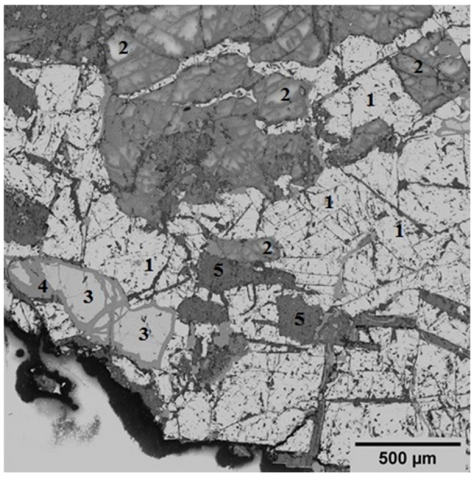

Figure 2. Specific electron microscopic image that showcases the structural details of an initial concentrate using back-scattered electrons (BSE). Symbols: 1—magnetite; 2—plagioclase; 3—ilmenite; 4—sphene; 5—tremolite.

The phase composition of the initial concentrate, as depicted in Figure 3, indicates that magnetite is the dominant mineral present. Additionally, the presence of tremolite and chlorite-serpentine indicates that there are also silicate minerals involved. The minor quantity of ilmenite suggests that titanium is also present in the concentrate.

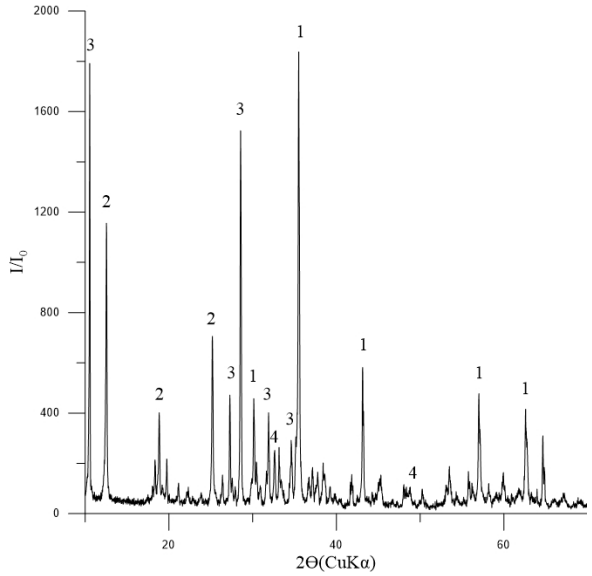

Figure 3. Diffractogram of the initial concentrate: 1—Fe_3O_4 (magnetite) [01-088-0315]; 2—$(Mg,Al)_6(Si,Al)_4O_{10}(OH)_8$ (chlorite-serpentine) [00-052-1044]; 3—$Ca_2Mg_5Si_8O_{22}(OH)_2$ (tremolite) [00-013-0437]; 4—$FeTiO_3$ (ilmenite) [01-075-0519].

The principal phase in the concentrates is magnetite, with tremolite, chlorite-serpentine, and trace amounts of ilmenite also present (Figure 4).

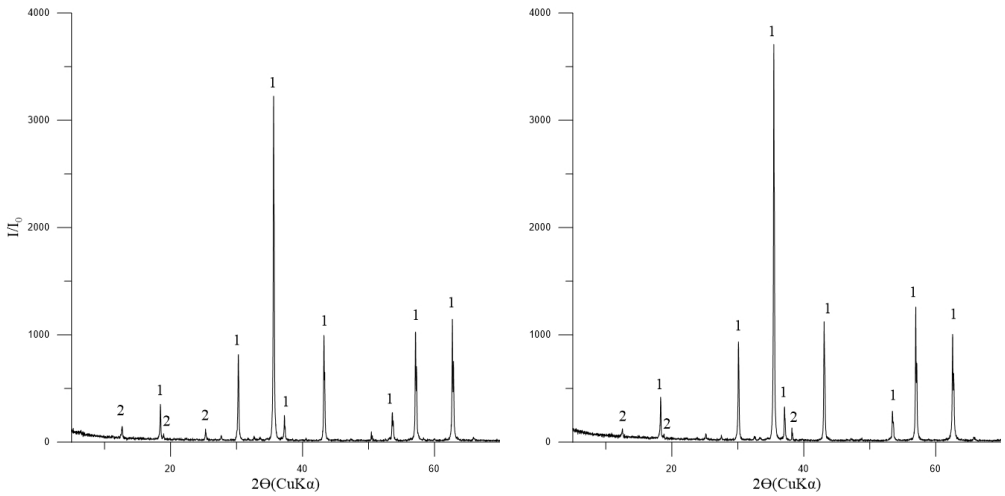

Figure 4. Diffractogram of the concentrates No. 1 (**a**) and 2 (**b**). Symbols: 1—Fe_3O_4 (magnetite) [01-088-0315]; 2—$(Mg,Al)_6(Si,Al)_4O_{10}(OH)_8$ (chlorite-serpentine) [00-052-1044]; $FeTiO_3$ (ilmenite) [01-075-0519].

The investigation into the particle size and shape of concentrates No. 1 and No. 2 yielded the following findings (Figure 5). The abscissa axis (xc_min) represents particle size in millimeters, while the ordinate axis (q3) depicts particle distribution density as a percentage per millimeter.

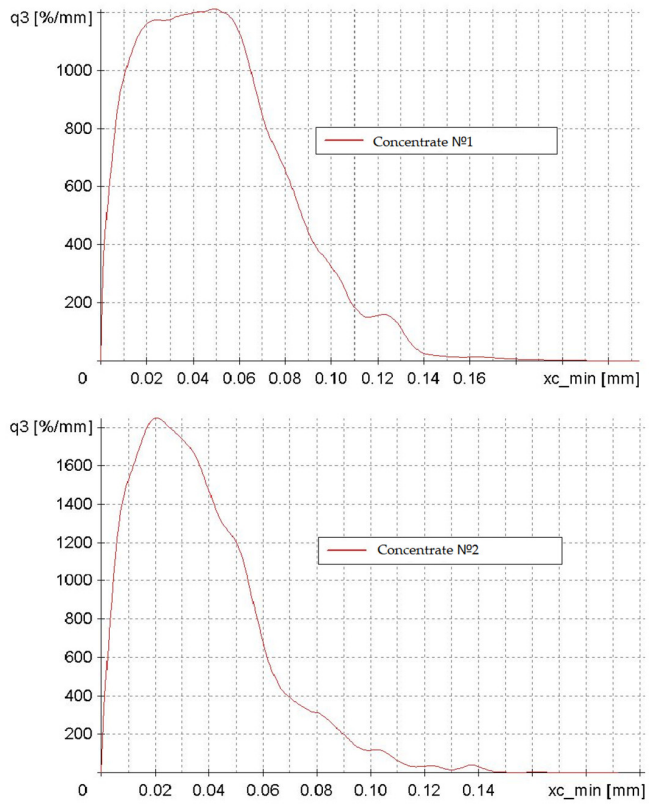

Figure 5. Particle distribution density plots of concentrates No. 1 and No. 2, categorized by particle size from 0 to 0.15 mm.

The two graphs illustrate a modal distribution with negative asymmetry, indicating that the predominant particle size of the concentrate is 0.02–0.05 mm. The particle size distribution of Concentrate No. 1 is more heterogeneous, featuring a broader range of particle sizes and a less distinct peak. The maximum density of the distribution is characteristic of Concentrate No. 2. This discrepancy can be attributed to the different enrichment methodologies employed in the initial preparation of the low-grade concentrate.

Figure 6 presents the findings from the image of the sample of Concentrate No. 2 (the studied large particle grains are marked with numbers) and the spectra of individual elements converted to oxides. Iron is converted to FeO, as specified in the software SEMVIEW 8000, while the remaining elements are converted to standard oxides.

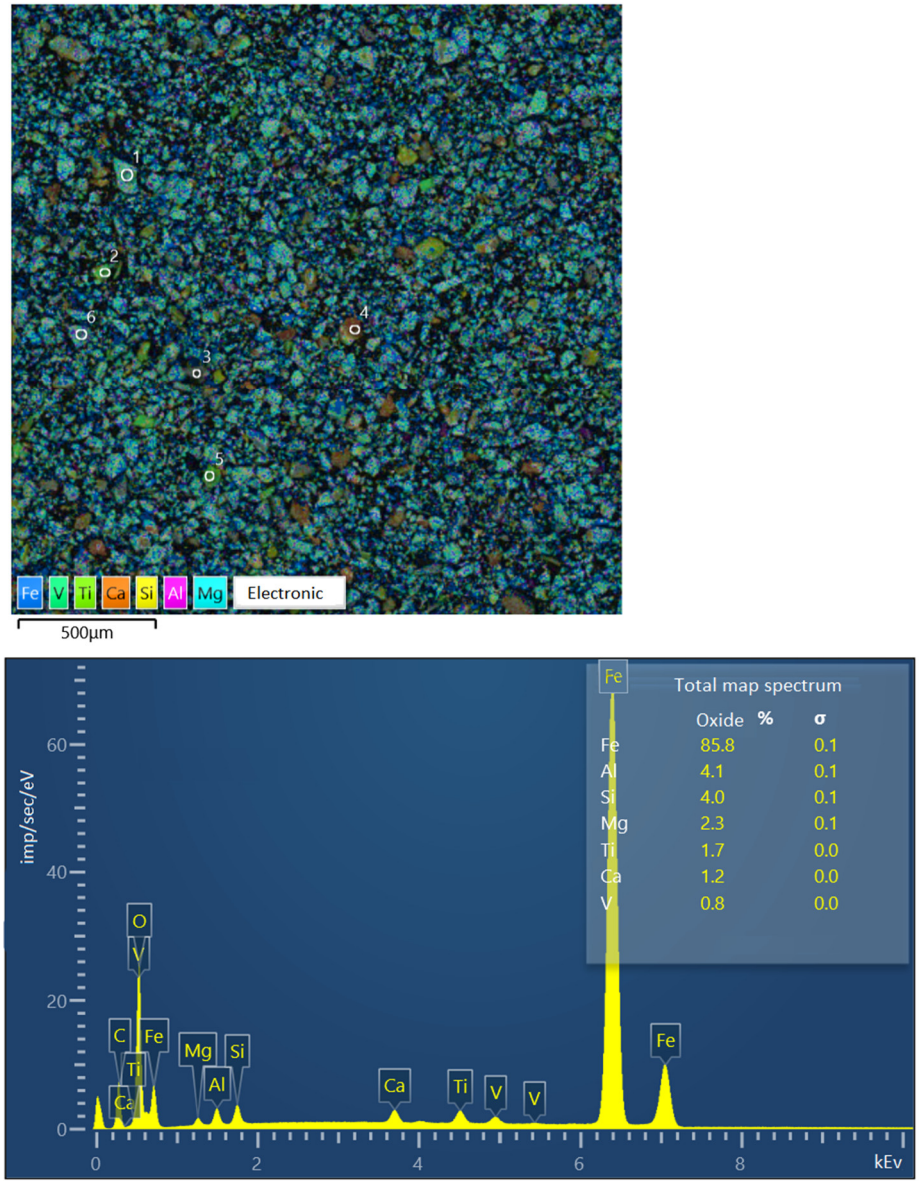

Figure 6. Image of concentrate sample No. 2 and elemental spectra.

The study focused on examining a series of large grains, measuring approximately 0.071 mm in size. The grains were classified into four categories (see image on the Figure 6, symbols from 1 to 6):

1. A titanomagnetite particle with ilmenite ingrowth.
2. A particle of presumably pure ilmenite.
3. A poorly formed particle, exhibiting a sprout structure and comprising 19.36% Fe.

4. A rock particle, comprising 5.64% Fe.
5. A particle of presumably pure ilmenite.
6. A particle of presumably pure titanomagnetite.

Table 4 presents the results of the elemental composition determination of the concentrate sample of improved quality and the individual large grains contained therein. Additionally, the table presents the findings of the chemical analysis of titanomagnetite grains, representing the physically separated monomineral fraction of titanomagnetite.

Table 4. Elemental composition of concentrate sample and individual grains according to electron microscopy data.

Content, at. %												
Fe_{total}	FeO	Fe_2O_3	MgO	Al_2O_3	SiO_2	CaO	TiO_2	V_2O_5	MnO	Ni	Co	Losses During Calcination
Total sample of enhanced concentrate												
66.73	–	–	2.33	4.14	4.03	1.16	1.68	0.82	–	–	–	–
4—rock particle (5.64% Fe)												
5.64	–	–	0.37	30.19	40.87	21.14	–	0.17	–	–	–	–
3—poor particle: titanomagnetite aggregate with rock minerals (19.36% Fe)												
19.36	–	–	22.58	21.39	29.64	0.67	0.69	–	0.12	–	–	–
2 and 5—particles of presumably pure ilmenite												
36.97	47.56	–	–	0.61	0.46	–	49.08	–	2.28	–	–	–
38.39	49.39	–	–	0.61	0.26	–	46.45	0.72	2.57	–	–	–
1—titanomagnetite particle with ilmenite ingrowth												
67.01	–	–	1.91	5.09	0.33	–	5.03	1.09	0.33	–	–	–
6—particle of presumably pure titanomagnetite												
68.88	–	–	–	7.58	0.36	–	2.00	1.24	0.20	–	–	–
Monomineral fraction of titanomagnetite												
68.32	31	63.5	0.35	1.3	0.1	0.1	2.9	0.88	0.16	0.01	0.012	0.3

The iron content of the concentrate, as determined by electron microscopy, was found to be 68.73%, which is in close agreement with the results of the chemical analysis (68.5% Fe).

The chemical composition of the pellets obtained is presented in Table 5.

Table 5. Chemical composition of laboratory pellets No. 1 and No. 2.

Sample	Content, Mass.%										
	Fe_{total}	Fe_{met}	FeO	CaO	SiO_2	Al_2O_3	MgO	MnO	TiO_2	V_2O_5	S
Pellets No. 1	64.58	-	1.20	1.328	1.76	1.63	0.91	0.087	1.47	0.70	0.006
Pellets No. 2	67.49	-	<1.00	1.200	0.73	1.22	0.66	0.080	1.24	0.70	0.003

The analysis of the pellets reveals that hematite is the principal mineral present, with minor components including Mg_2SiO_4 and $CaSiO_3$ (Figure 7).

In pellet No. 1, hematite (1) is the dominant phase, accompanied by a small amount of complex silicoferrite (2), specifically $Ca_{4.2}Mg_4Fe_{10.3}Si_{9.5}O_{40}$. This is visually represented in Figure 8a.

For pellet No. 2, the mineralogical composition is detailed in Figure 8b,c. This pellet also prominently features hematite, as indicated by the spectra labeled (83, 84, 89–95), and (101–103). Additionally, there is a minor presence of Fe_2TiO_5, known as pseudobrookite, which can be identified in spectra (85–88, 96–99), and (104).

The findings suggest that the firing conditions applied during the processing of these pellets led to the complete oxidation of magnetite to hematite, resulting in the observed mineralogical compositions.

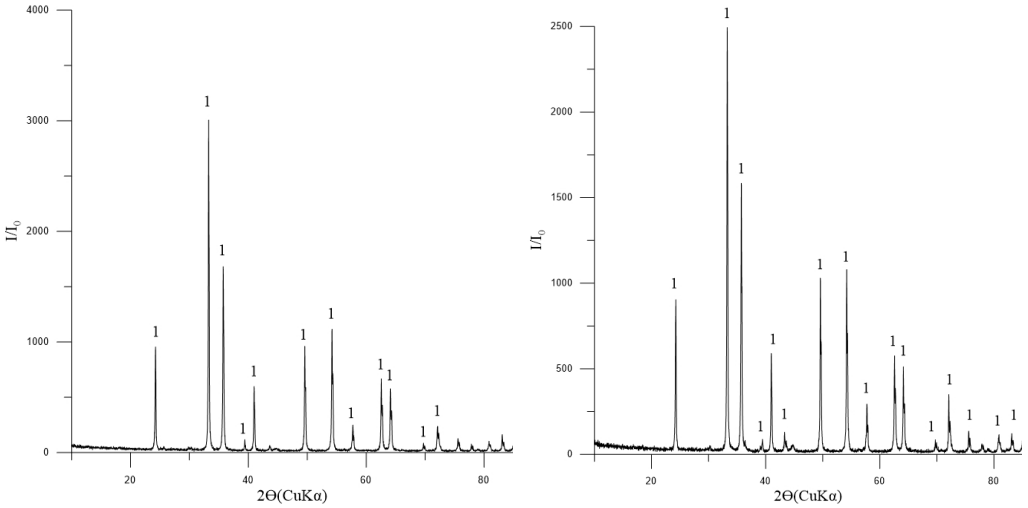

Figure 7. Diffractogram: (**a**) pellets No. 1; (**b**) pellets No. 2. Symbols: 1—Fe_2O_3 (hematite) [01-071-5088], minimum of Mg_2SiO_4 [01-075-1450] and $CaSiO_3$ [01-075-4984].

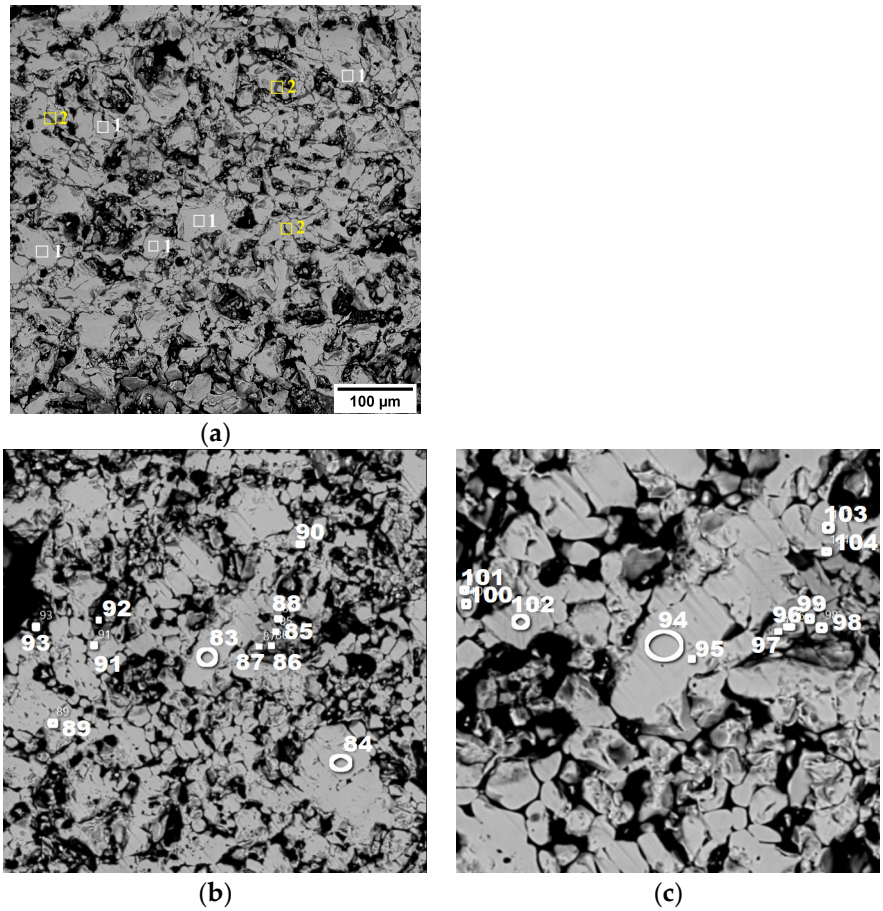

Figure 8. Structure of pellets No. 1 (**a**) and No. 2 (**b**,**c**) (in back-reflected electrons) at magnifications of 100× (**a**), 50× (**b**,**c**).

One of the crucial metallurgical attributes of pellets is their compressive strength. The compressive strength of annealed pellets exhibits considerable variation between different manufacturers, with reported values ranging from 150 to 300 kg/pellet [27,28].

Given the significant alteration in the contact area between the deformed pellet and the testing apparatus during compression testing, it is not appropriate to utilize destructive nor-

mal contact stress as a representative characteristic of strength, as is the case in compression tests of cylindrical specimens. Furthermore, the results of mathematical modeling [29,30] indicate that the most unfavorable stress state in the compression of spherical-shaped pellets occurs in the center due to the action of intense tensile radial stresses.

Consequently, the magnitude of the breaking force in compression tests is typically employed as a metric for assessing the strength of pellets. Nevertheless, a number of authors (e.g., [31]) posit that the compressive fracture energy is a more representative indicator of pellet strength. This is because the energy criteria of strength, in contrast to the force criteria, permit consideration of the dissipation of energy during the plastic deformation of the material.

In its initial unburnt state, the pellet is composed of iron ore magnetite concentrate and a binder, namely bentonite. Upon firing, the magnetite is oxidized, resulting in the formation of hematite, which represents the active phase. As a consequence of the sintering of the hematite grains, the strength characteristics are enhanced [32]. If the process of magnetite oxidation has occurred completely over the entire cross-section of the pellets, the resulting structure will be homogeneous and composed of hematite.

In industrial conditions, pellets are roasted at temperatures of 1250–1350 °C, with a typical heating rate of 100 °C/min or higher. At such firing parameters, complete oxidation of magnetite does not occur, and pellets typically exhibit a zonal structure [33–36] comprising a magnetite core and a hematite shell, thereby displaying a pronounced two-phase structure. The disparity in temperature between the magnetite and hematite zones of zonal pellets, which undergo a transition from a plastic to an elastic state, is accompanied by a notable contraction and a variety of alterations in their dimensions. This phenomenon gives rise to the emergence of internal stresses at the interface between the magnetite and hematite zones [37].

The results of the compression tests conducted on pellets No. 1 and No. 2 are presented in Figure 9a and Figure 9b, respectively.

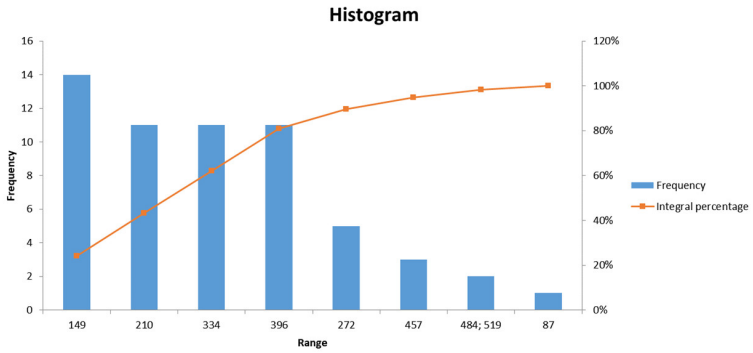

(**a**)

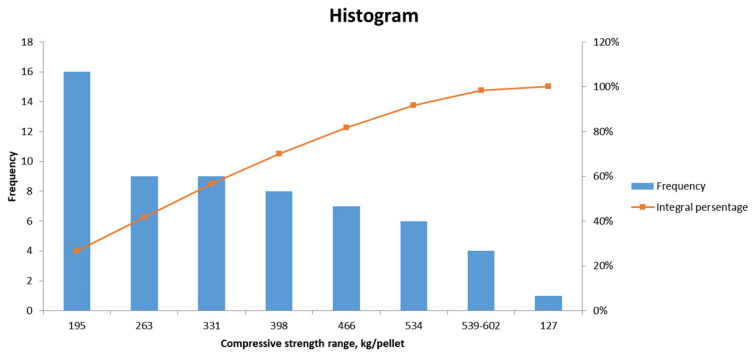

(**b**)

Figure 9. Frequency distribution graph of compressive strength values of pellets No. 1 (**a**), pellets No. 2 (**b**).

The average strength of laboratory pellets No. 1 (for blast furnace production) is 246.6 kg/pellet, with a minimum of 78 kg/pellet, a maximum of 519 kg/pellet, a median of 240 kg/pellet, and a mode of 320 kg/pellet. The requisite compressive strength of pre-main unfluxed pellets is greater than 220 kg/pellet.

The average strength of laboratory pellets No. 2 (for metallization) is 312.6 kg/pellet, with a minimum of 127 kg/pellet, a maximum of 602 kg/pellet, a median of 295 kg/pellet, and a mode of 252 kg/pellet. The requisite compressive strength of non-fluxed pellets for metallization is greater than 300 kg/pellet.

A study was conducted to examine the reducibility of pellets No. 1 (for blast furnace production). The chemical composition of the reduced pellets is as follows: the total iron content was found to be 76.29%, with the iron oxide accounting for 40.46% and the metallic iron component representing 40.34%. The phase composition of reduced pellets No. 1 is presented in Figure 10.

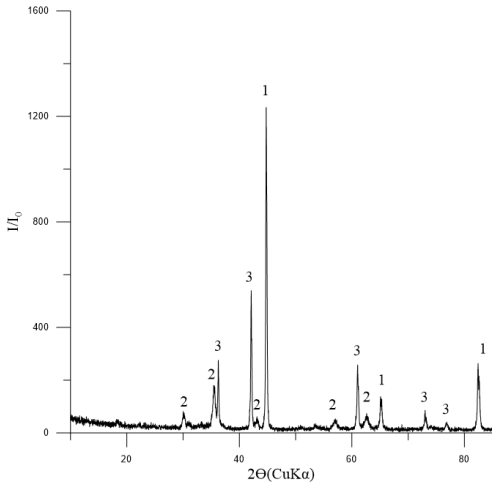

Figure 10. Diffractogram of reduced pellets No. 1: 1—Fe_{met} [01-076-6587]; 2—Fe_3O_4 (magnetite) [01-088-0315]; 3—FeO (wüstite) [01-077-7981].

The macrostructure of the reduced pellet is illustrated in Figure 11. It can be observed that the reducing of the pellet occurs in a manner that progresses from the surface to the depth. The absolute degree of reducing by chemical analysis (R1) was 66.56%, while the absolute degree of reducing by mass loss (R2) was 63.38%. The actual degree of reducing (R_{fact}) was 66.4%. It is recommended that the reducing rate for pellets should be above 80%. The reducibility of pellet No. 1 is below the recommended threshold, which is to be expected given the low porosity and strength of the pellets. There is an inverse relationship between the strength of iron ore materials and reducibility, whereby an increase in one parameter is accompanied by a decrease in the other [38].

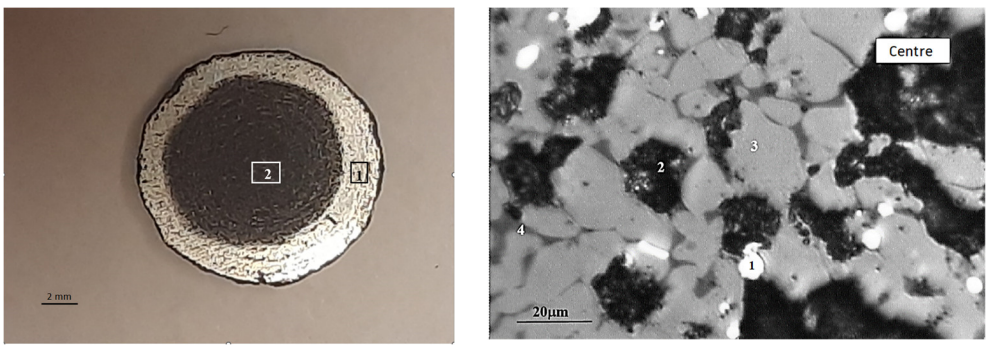

Figure 11. Typical macrostructure of reduced BF pellets: **left** (1—edge, 2—center), **right** (in the center: 1—Fe_{met}; 2—pores; 3—magnetite; 4—FeO).

The low-temperature fracture index ($LTD_{+6.3}$) was found to be 37.2%, which is an unsatisfactory result for pellets. It is recommended that the LTD index should be above 60%. The low value of hot strength can be attributed to the insufficient presence of binding oxides in the concentrate, such as CaO, SiO_2, MgO, and Al_2O_3, which are essential for imparting thermomechanical strength [39–42].

The softening temperature range is 100 °C (1160–1260 °C), representing an average value for the temperature range typically observed in blast furnaces.

Table 6 presents the chemical composition of pellets No. 2 following metallization at 3 and 4 h of exposure. The degree of metallization is calculated as the ratio of metallic iron to total iron, expressed as a percentage. In order to facilitate electrowinning, the metallization degree must exceed 88%.

Table 6. Chemical composition of metalized pellets.

Time of Exposure	Content, Mass. %			Degree of Metallization, %
	Fe_{total}	FeO	Fe_{met}	
3 h	83.53	7.34	72.02	86.22
4 h	85.00	0.10	78.62	92.50

The phase composition of the metallized pellets is shown in Figure 12a,b.

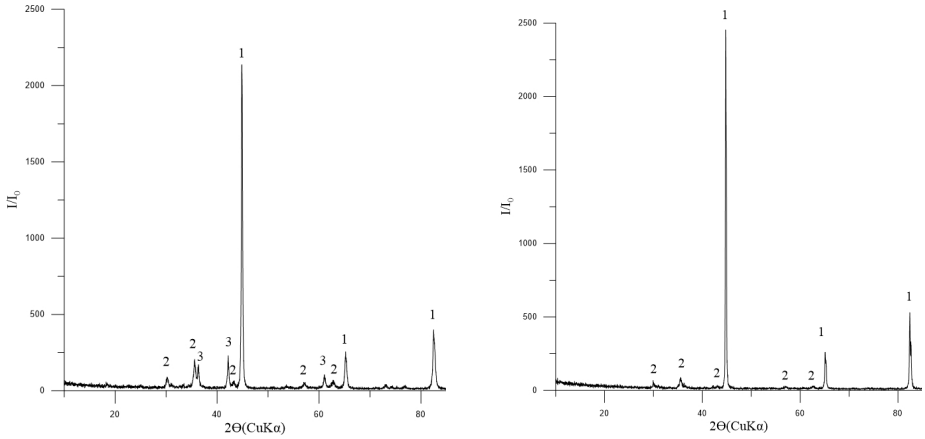

Figure 12. Diffractogram of metallized pellets No. 2: (**a**) 3 h of exposure; (**b**) 4 h of exposure: 1—Fe_{met} [01-076-6587]; 2—Fe_3O_4 (magnetite) [01-088-0315]; 3—FeO (wüstite) [01-077-7981].

The macrostructure of the metallized pellets is shown in Figure 13.

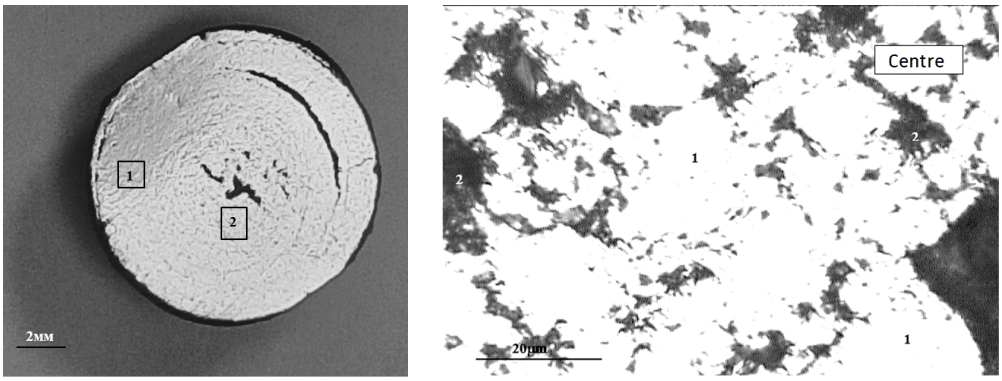

Figure 13. Typical macrostructure of metallized pellets: **left** (1—edge, 2—center), **right** (in the center: 1—Fe_{met}; 2—pores).

4. Conclusions

The following results were obtained from the study.

The chemical, phase, and mineralogical compositions of concentrates of standard (64.5% Fe) and upgraded (68.5% Fe) quality from the Pervouralskoye deposit were analyzed. The principal phase identified in the concentrates is magnetite, with tremolite, chlorite-serpentine, and a minor quantity of ilmenite also present.

Under laboratory conditions, pellets of standard and superior quality were produced and subjected to combustion. The principal phase present in the pellets was hematite.

The compressive strength of both types of annealed pellets was evaluated. For pellets intended for blast furnace production (standard, No. 1), the average compressive strength was 247 kg/pellet, which complies with the requirements for blast furnace production. For pellets designed for metallization (superior quality, No. 2), the average compressive strength was 313 kg/pellet, which complies with the requirements for the metallization process.

The metallurgical properties of pellet No. 1 were investigated. The actual reducing degree (R_{fact}) was found to be 66.4%, which is below the recommended value for blast furnace production. Similarly, the low-temperature disintegration index $LTD_{+6.3}$ was determined to be 37.2%, again falling below the recommended value for blast furnace production. However, the softening temperature range was found to be 100 °C, which meets the requirements for blast furnace production. To impart the requisite metallurgical characteristics to the pellets, it is advisable to test a variety of firing modes and to incorporate a greater proportion of binding materials into the charge prior to pelletization, thereby enhancing the strength of the material.

The degree of metallization of annealed pellets No. 2, following restoration by gas with a composition of $CO + N_2$ (90/10%), after 3 h and 4 h exposures, was investigated. The results demonstrate that the optimal degree of metallization was achieved with a four-hour exposure, reaching 92.5%. This level of metallization aligns with the requirements for electric steelmaking production.

Author Contributions: Conceptualization A.N.D.; synthesis of samples E.A.V., R.V.A. and V.V.K.; Supervision G.Y.V. and L.A.M.; writing—original draft preparation G.Y.V. and Y.E.B.; writing—review and editing, G.Y.V. and V.G.Z.; Resources R.V.A. and L.A.M.; Validation, A.N.D. and V.G.Z. All authors have read and agreed to the published version of the manuscript.

Funding: The project was supported by the State Assignment of the Institute of Metallurgy of the Ural Branch of the Russian Academy of Sciences within the Program of Fundamental Research of State Academies.

Institutional Review Board Statement: Not applicable.

Informed Consent Statement: Not applicable.

Data Availability Statement: The original contributions presented in this study are included in the article. Further inquiries can be directed to the corresponding author.

Acknowledgments: The authors would like to express their gratitude to A.E. Pelevin for the invaluable advice and assistance provided.

Conflicts of Interest: The authors declare no conflicts of interest.

References

1. Global DRI Output up 9.8 Percent in May. Available online: https://www.steelorbis.com/steel-news/latest-news/global-dri-output-up-98-percent-in-may-1345780.htm (accessed on 19 September 2024).
2. Kurunov, I.F. The direct production of iron and alternatives to the blast furnace in iron metallurgy for the 21st century. *Metallurgist* **2010**, *54*, 335–342. [CrossRef]
3. Battle, T.; Srivastava, U.; Kopfle, J.; Hunter, R.; McClelland, J. The Direct Reduction of Iron. In *Treatise on Process Metallurgy*; Elsevier: Amsterdam, The Netherlands, 2024; pp. 89–149. [CrossRef]
4. Hasanbeigi, A.; Arens, M.; Price, L. Alternative Emerging Ironmaking Technologies for Energy-Efficiency and Carbon Dioxide Emissions Reduction: A Technical Review. *Renew. Sustain. Energy Rev.* **2014**, *33*, 645–658. [CrossRef]

5. Sah, R.; Dutta, S. Direct Reduced Iron: Production. In *Encyclopedia of Iron, Steel, and Their Alloys*; Taylor and Francis: New York, NY, USA, 2016; pp. 1082–1108. [CrossRef]
6. AbdElmomen, S.S. Reoxidation of direct reduced iron in ambient air. *Ironmak. Steelmak.* **2014**, *41*, 107–111. [CrossRef]
7. Sahu, S.N.; Baskey, P.K.; Barma, S.D.; Sahoo, S.; Meikap, B.C.; Biswal, S.K. Pelletization of synthesized magnetite concentrate obtained by magnetization roasting of Indian low-grade BHQ iron ore. *Powder Technol.* **2020**, *374*, 190–200. [CrossRef]
8. Ramakgala, C.; Danha, G. A review of ironmaking by direct reduction processes: Quality requirements and sustainability. *Procedia Manuf.* **2019**, *35*, 242–245. [CrossRef]
9. Liu, J.; Xing, Z.; Wang, X.; Cheng, G.; Xue, X. Effect of V_2O_5 on Consolidation, Reduction, and Softening-Melting Behavior of High-Cr Vanadium Titanomagnetite. *Metals* **2023**, *13*, 1171. [CrossRef]
10. Peng, Z.; Wang, Z.; Han, Z.; Zhu, Y.; Li, Y.; Xie, K. Vanadium–Titanium Magnetite Concentrate, Calcium-Magnesium Composite Roasting and Sulfuric Acid Leaching for Vanadium Extraction from Pellets. *Metals* **2023**, *13*, 1135. [CrossRef]
11. Wei, R.F.; Li, J.X.; Tang, G.W.; Cang, D.Q. Strength and consolidation mechanism of iron ore and coal pellets. *Ironmak. Steelmak.* **2014**, *41*, 514–520. [CrossRef]
12. Kawatra, S.K.; Claremboux, V. Iron Ore Pelletization: Part II. Inorganic Binders. *Miner. Process. Extr. Metall. Rev.* **2021**, *43*, 813–832. [CrossRef]
13. Bulatov, K.V.; Gazaleeva, G.I. The metallization process of titanium magnetite. *AIP Conf. Proc.* **2022**, *2456*, 020012. [CrossRef]
14. Sun, Y.; Zheng, H.; Dong, Y.; Jiang, X.; Shen, Y.; Shen, F. Melting and separation behavior of slag and metal phases in metallized pellets obtained from the direct-reduction process of vanadium-bearing titanomagnetite. *Int. J. Miner. Process.* **2015**, *142*, 119–124. [CrossRef]
15. Xin, J.; Wang, N.; Chen, M.; Chen, C. Slag-metal Separation and Reduction Behaviors of Vanadium-bearing Titanomagnetite Metallized Pellets. *ISIJ Int.* **2020**, *60*, 823–831. [CrossRef]
16. Sui, Y.; Guo, Y.; Jiang, T.; Qiu, G. Separation and recovery of iron and titanium from oxidized vanadium titano-magnetite by gas-based reduction roasting and magnetic separation. *J. Mater. Res. Technol.* **2019**, *8*, 3036–3043. [CrossRef]
17. Chen, J.; Chen, W.; Mi, L.; Jiao, Y.; Wang, X. Kinetic Studies on Gas-Based Reduction of Vanadium Titano-Magnetite Pellet. *Metals* **2019**, *9*, 96. [CrossRef]
18. Wang, S.; Guo, Y.; Jiang, T.; Yang, L.; Chen, F.; Zheng, F.; Xie, X.; Tang, M. Reduction Behaviors of Iron, Vanadium and Titanium Oxides in Smelting of Vanadium Titanomagnetite Metallized Pellets. *JOM* **2017**, *69*, 1646–1653. [CrossRef]
19. Feng, C.; Chu, M.; Tang, J.; Liu, Z. Effects of smelting parameters on the slag/metal separation behaviors of Hongge vanadium-bearing titanomagnetite metallized pellets obtained from the gas-based direct reduction process. *Int. J. Miner. Metall. Mater.* **2018**, *25*, 609–622. [CrossRef]
20. Wang, S.; Guo, Y.; Zheng, F.; Chen, F.; Yang, L.; Chen, M.; Zhao, B.; Jiang, T. Optimization of Basicity of High Ti Slag for Efficient Smelting of Vanadium Titanomagnetite Metallized Pellets. *Metall. Mater. Trans. B* **2020**, *51*, 945–952. [CrossRef]
21. Shi, Y.; Guo, Z.; Zhu, D.; Pan, J.; Lu, S. Isothermal reduction kinetics and microstructure evolution of various vanadium titanomagnetite pellets in direct reduction. *J. Alloys Compd.* **2023**, *953*, 170126. [CrossRef]
22. Shi, Y.; Zhu, D.; Pan, J.; Guo, Z.; Lu, S.; Xue, Y. Investigation into the coal-based direct reduction behaviors of various vanadium titanomagnetite pellets. *J. Mater. Res. Technol.* **2022**, *19*, 243–262. [CrossRef]
23. Tang, W.; Yang, S.; Yang, H.; Xue, X. Effect of Co_2O_3 on Oxidation Induration and Reduction Swelling of Chromium-Bearing Vanadium Titanomagnetite Pellets with Simulated Coke Oven Gas. *Metals* **2019**, *9*, 16. [CrossRef]
24. Fan, W.; Peng, Z.; Tian, R.; Luo, G.; Yi, L.; Rao, M. Toward Metallized Pellets for Steelmaking by Hydrogen Cooling Reduction: Effect of Gas Flow Rate. *Materials* **2024**, *17*, 3896. [CrossRef] [PubMed]
25. Luo, G.; Peng, Z.; Gao, K.; Fan, W.; Tian, R.; Yi, L.; Rao, M. Preparation of Metallized Pellets for Steelmaking by Hydrogen Cooling Reduction with Different Cooling Rates. *Materials* **2024**, *17*, 4362. [CrossRef] [PubMed]
26. Lv, C.; Bai, S. Upgrading of raw vanadium titanomagnetite concentrate. *J. S. Afr. Inst. Min. Metall.* **2019**, *119*, 11. [CrossRef] [PubMed]
27. Eklund, N.; Dahlstedt, A. The choice of pellets in a mixed blast furnace burden and how it effects process conditions. In Proceedings of the 14th Conference on Hungarian Pig Iron and Steel Making—2002, Balatonszeplak, Lulea, Sweden, 12–13 September 2002; pp. 1–14.
28. Gao, Q.; Shen, F.; Wei, G.; Jiang, X.; Zheng, H. Effects of MgO containing additive on low-temperature metallurgical properties of oxidized pellet. *J. Iron Steel Res. Int.* **2013**, *20*, 25–28. [CrossRef]
29. Gustafsson, G.; Häggblad, H.-A.; Nishida, M.; Larsson, S.; Jonsén, P. Fracture probability modelling of impact-loaded iron ore pellets. *Int. J. Impact Eng.* **2017**, *102*, 180–186. [CrossRef]
30. Gustafsson, G.; Häggblad, H.-A.; Jonsén, P. Multi-particle finite element modelling of the compression of iron ore pellets with statistically distributed geometric and material data. *Powder Technol.* **2013**, *239*, 231–238. [CrossRef]
31. Tavares, L.M.; Cavalcanti, P.P.; de Carvalho, R.M.; da Silveiera, M.W.; Bianchi, M.; Otaviano, M. Fracture probability and fragment size distribution of fired Iron ore pellets by impact. *Powder Technol.* **2018**, *336*, 546–554. [CrossRef]
32. Yur'ev, B.P.; Goltsev, V.A. Oxidation of magnetite. *Steel Transl.* **2016**, *46*, 718–721. [CrossRef]
33. Dwarapudi, S.; Devi, T.U.; Mohan, R.S.; Ranjan, M. Influence of pellet size on quality and microstructure of iron ore pellets. *ISIJ Int.* **2008**, *48*, 768–776. [CrossRef]

34. Umadevi, T.; Kumar, P.; Lobo, N.F.; Prabhu, M.; Mahapatra, P.C.; Ranjan, M. Influence of pellet basicity (CaO/SiO_2) on iron ore pellet properties and microstructure. *ISIJ Int.* **2011**, *51*, 14–20. [CrossRef]
35. Gao, Q.; Shen, Y.; Jiang, X.; Shen, F.; Liu, C. Effect of MgO on oxidation process of Fe_3O_4 in pellets. *J. Iron Steel Res. Int.* **2016**, *23*, 1007–1011. [CrossRef]
36. Odo, J.; Nwoke, V. Effect of Core Diameter on the Compressive Strength and Porosity of Itakpe Iron Ore Pellets. In *10th International Symposium on High-Temperature Metallurgical Processing*; The Minerals, Metals & Materials Series; Springer: Cham, Switzerland, 2019; pp. 511–521. [CrossRef]
37. Melamud, S.G.; Yur'ev, B.P. Stress calculation in roasted iron ore pellets on cooling. *Steel Transl.* **2015**, *45*, 903–907. [CrossRef]
38. Dmitriev, A.N.; Vitkina, G.Y.; Chesnokov, Y.A. Methodical basis of investigation of influence of the iron ore materials and coke metallurgical characteristics on the blast furnace smelting efficiency. *Adv. Mater. Res.* **2013**, *602–604*, 365–375. [CrossRef]
39. Dmitriev, A.N.; Vyaznikova, E.A.; Vitkina, G.Y.; Karlina, A.I. A Study of the Structure and Physicochemical Properties of the Mixed Basicity Iron Ore Sinter. *Magnetochemistry* **2023**, *9*, 212. [CrossRef]
40. Iljana, M.; Paananen, T.; Mattila, O.; Kondrakov, M.; Fabritius, T. Effect of Iron Ore Pellet Size on Metallurgical Properties. *Metals* **2022**, *12*, 302. [CrossRef]
41. Kotta, A.B.; Karak, S.K.; Kumar, M. Effect of mineralogy on reduction behaviour of iron ore pellets. *Mater. Sci. Forum* **2020**, *978*, 525–531. [CrossRef]
42. Yi, L.; Huang, Z.; Jiang, T.; Zhong, R.; Liang, Z. Iron ore pellet disintegration mechanism in simulated shaft furnace conditions. *Powder Technol.* **2017**, *317*, 89–94. [CrossRef]

Disclaimer/Publisher's Note: The statements, opinions and data contained in all publications are solely those of the individual author(s) and contributor(s) and not of MDPI and/or the editor(s). MDPI and/or the editor(s) disclaim responsibility for any injury to people or property resulting from any ideas, methods, instructions or products referred to in the content.